RESEARCH ARTICLE
doi.org/10.1002/elsa.202100096

Chemistry Europe
European Chemical Societies Publishing

Received: 23 May 2021
Revised: 11 June 2021
Accepted: 21 June 2021

Electrochemical immunosensing of Growth arrest-specific 6 in human plasma and tumor cell secretomes

Cristina Muñoz-San Martín[1] | **Víctor Pérez-Ginés**[1] | **Rebeca M. Torrente-Rodríguez**[1] | **Maria Gamella**[1] | **Guillermo Solís-Fernández**[2] | **Ana Montero-Calle**[2] | **María Pedrero**[1] | **Verónica Serafín**[1] | **Neus Martínez-Bosch**[3] | **Pilar Navarro**[3,4,5] | **Pablo García de Frutos**[4,5] | **Montserrat Batlle**[5,6] | **Rodrigo Barderas**[2] | **José M. Pingarrón**[1] | **Susana Campuzano**[1]

[1] Departamento de Química Analítica, Facultad de CC. Químicas, Universidad Complutense de Madrid, Madrid, Spain

[2] Chronic Disease Programme, UFIEC, Carlos III Health Institute, Majadahonda, Madrid, Spain

[3] Cancer Research Program, Hospital del Mar Medical Research Institute (IMIM), Unidad Asociada IIBB-CSIC, Barcelona, Spain

[4] Departamento de Muerte y Proliferación Celular, Instituto de Investigaciones Biomédicas de Barcelona – Centro Superior de Investigaciones Científicas (IIBB-CSIC), Barcelona, Spain

[5] Institut d'Investigacions Biomèdiques August Pi i Sunyer (IDIBAPS), Barcelona, Catalonia, Spain

[6] Centro de Investigación Biomédica en Red de Enfermedades CardioVasculares (CIBERCV), Instituto de Carlos III, Madrid, Spain

Correspondence
María Pedrero and Susana Campuzano, Departamento de Química Analítica, Facultad de CC. Químicas, Universidad Complutense de Madrid, E-28040, Madrid, Spain.
Email: mpedrero@quim.ucm.es; susanacr@quim.ucm.es

Abstract

Growth arrest-specific 6 (GAS6) protein plays a key role in processes related to proliferation, inflammation, angiogenesis, and atherosclerotic plaque formation. In addition, it has been reported that plasma levels of GAS6 are related to cancer prognosis and other relevant pathologies, such as heart failure or sepsis. We report here the first electrochemical immunoplatform for the determination of GAS6, which has demonstrated to be competitive with other available methodologies in terms of cost, simplicity, and decentralized application. The developed immunoplatform involves a sandwich immunoassay using magnetic microparticles (MBs) and uses amperometric detection at disposable screen-printed carbon electrodes (SPCEs). The MBs were modified with an antibody specific to GAS6 for its selective capture, which is further recognized by a biotinylated secondary antibody subsequently labeled with a streptavidin-horseradish peroxidase (Strep-HRP) conjugate. The electrochemical detection was carried out using the hydroquinone (HQ)/H_2O_2 system. The developed bioplatform exhibits a great selectivity and low limit of detection (27 pg/mL) that allowed the determination of the GAS6 circulating level in plasma samples from patients suffering heart failure (HF) and diagnosed with pancreatic ductal adenocarcinoma (PDAC), as well as the determination of the target protein in raw secretomes of human colorectal cancer cell lines.

KEYWORDS
amperometric, GAS6, immunosensor, plasma, secretome

RESEARCH ARTICLE
doi.org/10.1002/elsa.202100096
Chemistry Europe
European Chemical Societies Publishing

1 | INTRODUCTION

Biomarkers can be used for a better understanding of fundamental biological processes, providing information on what is happening in a cell or an organism at a given moment and thus serving as early warnings for health monitoring.

Growth arrest-specific 6 (GAS6) protein has been proposed as an important factor in some complex pathological processes.[1] GAS6 was originally isolated as the product of growth arrest-specific gene 6 and belongs to the vitamin K-dependent proteins (VKDPs) family. GAS6 exerts its effects by binding TYRO3, Axl, and Mer receptor tyrosine-kinases (TAM family), showing the highest affinity for Axl.[2] It is mainly expressed in the lungs, heart, kidneys, intestine, bone marrow, vascular smooth muscle cells, monocytes and, at very low levels, in the liver,[3] and the GAS6 plasma concentration is much lower than that other VKDPs.[4] It has been reported that GAS6 plays key roles in several biological processes including proliferation, migration, differentiation, and adhesion, leukocyte sequestration, platelet aggregation and hematopoiesis, apoptosis, and phagocytosis, and that it is generally associated with conditions of injury, inflammation, and repair.[3,5]

The GAS6/TAM ligand/receptor system is involved in early immunomodulation,[6] regulating the immune response by modulating cytokine production, and inducing a regulatory cellular response.[7] In addition, it has been shown that the activation of the GAS6/TAM signaling pathway plays an important role in the generation and progression of a wide variety of cancers due to its implication in cell growth and proliferation. Specifically, GAS6 is overexpressed in melanoma, schwannoma, glioma, and pancreatic ductal adenocarcinoma cell lines.[8–12] Moreover, it is upregulated in ovarian cancer,[13,14] and there are studies on the mechanism of GAS6 expression in malignant breast processes.[15,16] Clinically, high expression of GAS6 is considered as an independent prognostic factor for poor survival in several cancers.[10,17]

In addition to the interest sparked by liquid biopsy in recent years, the cancer secretome, i.e., all the proteins released by cancer cells, is also garnering much attention and, although much less explored, is a promising and reliable source of cancer biomarkers. Secretome proteins play an important role in many essential physiological and pathophysiological processes, such as cell growth and differentiation, invasion, and metastasis via an endocrine, paracrine, or autocrine way.[18] Therefore, the analysis of cancer secretome is considered of high interest for the identification of candidate biomarkers, and to provide new insights into the molecular mechanisms of carcinogenesis by targeting altered molecules which are vital for cancer progression and metastasis.[19,20] Pancreatic ductal adenocarcinoma (PDAC) is one of the most aggressive tumors, with a 5-year survival rate less than 10 %.[21] Lack of validated biomarkers for early diagnosis is one of the main reasons for PDAC dismal prognosis and most of the patients are diagnosed at advanced stages, when they are not candidate for curative surgical resection.[22] Therefore, identification of novel PDAC *bona fide* biomarkers and diagnostic methods is an urgent need in pancreatic oncology.

GAS6 has also been described as novel key regulator of the vascular system due to its role in both inflammation and thrombosis, which are related events involved in many cardiovascular diseases repair.[3] After vascular damage, the platelets are activated to induce clot formation and repair the endothelium. GAS6 is secreted by endothelial cells upon damage[23] and TAM activation increases the expression of adhesion molecules such as VCAM-1 (vascular cell adhesion protein 1).[24] Additionally, it has been reported that GAS6 deficiency protects from thrombosis in mouse models,[23,24] and higher circulating GAS6 levels have been associated with thromboembolism.[25] Besides, GAS6/Axl system promotes the survival and proliferation of vascular smooth muscle cells and endothelial cells, leading to the formation of new vessels.[26] All these mechanisms have direct implications in cardiovascular diseases.[27,28]

Due to the key role of this biomarker in different diseases and seeking for alternative improved methods besides the routinely used sandwich ELISA to measure GAS6, we report the first electrochemical biosensing approach for the determination of GAS6. Electrochemical biosensors are a very interesting alternative to other technologies because of their inherent technical simplicity, affordable cost, sensitivity and selectivity, multiplexing ability, and adaptability for the fabrication of point-of-care (POC) devices.[29,30]

The strategy reported in this paper involves a protocol implemented on the surface of magnetic microbeads (MBs) and amperometric detection at unmodified screen-printed carbon electrodes (SPCEs). The method relies on the preparation of immunoconjugates on the surface of MBs, which were used to selectively capture and sandwich the GAS6 protein with specific antibodies further labeled with a streptavidin horseradish peroxidase (Strep-HRP) conjugate. The modified MBs were magnetically captured on the surface of the working SPCE and the activity of the HRP attached to the MBs was amperometrically measured at a potential of −0.20 V versus the Ag pseudoreference electrode, in the presence of H_2O_2 and hydroquinone (HQ). The immunoplatform was successfully applied to the analysis of GAS6 in human plasma samples from patients of heart failure (HF) or PDAC, as

RESEARCH ARTICLE
doi.org/10.1002/elsa.202100096
Chemistry Europe
European Chemical Societies Publishing

well as in secretomes of human colorectal cancer (CRC) cell lines.

2 | MATERIALS AND METHODS

2.1 | Apparatus and electrodes

A CHI1140A (CH Instruments, Inc.) potentiostat controlled by the software CHI1140A, and a Magellan V 7.1 (TECAN) ELISA plate reader were used to make the amperometric and spectrophotometric measurements, respectively. Screen-printed carbon electrodes (SPCEs) (DRP-110) and the specific cable connector (DRP-CAC) were purchased from Metrohm Hispania, S.L.U. Other instruments used were a Vortex (Velp Scientifica), a BioSan TS-100 constant temperature incubator shaker (Thermo), magnetic concentrators DynaMag®2 (Invitrogen – ThermoFisher Scientific), a magnetic stirrer (Inbea S.L.), and Basic pH-meter (Basic 20+, Crison). The capture of the modified MBs onto the SPCE surface was controlled by a neodymium magnet (AIMAN GZ) embedded in a homemade polymethacrylate (PMMA) casing.

2.2 | Reagents and solutions

Carboxylic acid-modified magnetic microbeads (HOOC-MBs, Dynabeads®, M-270) were purchased from Invitrogen-Thermo Fisher. Recombinant human GAS6 standard, goat anti-human GAS6 (CAb), and biotinylated goat anti-human GAS6 detector antibody (b-DAb) were purchased as an ELISA Kit (DuoSet®, DY885B, R&D Systems Europe, Ltd.). Blocker casein solution (BB solution: PBS containing 1 % w/v casein, pH 7.4) was purchased from Thermo Fisher Scientific, and sodium hydroxide (NaOH) from Labkem. Sodium chloride (NaCl), potassium chloride (KCl), sodium di-hydrogen phosphate dihydrate ($NaH_2PO_4 \times 2H_2O$) and anhydrous di-sodium hydrogen phosphate (Na_2HPO_4) were purchased from Scharlab. N-(3-dimethylaminopropyl)-N'-ethylcarbodiimide (EDC), N-hydroxysulfosuccinimide (sulfo-NHS), hydroquinone (HQ), hydrogen peroxide (H_2O_2) (30 %, w/v), ethanolamine, Tween® 20, human hemoglobin (Hb), human serum albumin (HSA), and IgG from human serum were purchased from Sigma–Aldrich. Streptavidin peroxidase conjugate (Strep-HRP) was purchased from Roche Diagnostics GmbH. Human NT-proBNP, human Axl, human HIF-1α, human interleukin-13 receptor α2 (IL-13Rα2), and human total E-cadherin (E-CDH) standards (DuoSet-IC, Catalog Number DY3604, DYC1643-2, DYC1935, DY614, and DYC4225, respectively, R&D Systems Europe, Ltd.), human lipoprotein a (Lp(a), from Abcam), recombinant human TNF-α protein from BD Pharmigen and recombinant human cadherin-17 (CDH-17) protein (OriGene Technologies, Inc.) were also used. GAS6 polyclonal antibody (Catalog Number E-AB-62753, Elabscience®) was used for Western blot (WB) analysis. All reagents were of the highest available grade.

The following buffer solutions, prepared with deionized water from a Milli-pore Milli-Q purification system (18.2 MΩ cm), were employed: 0.05 M phosphate buffer, pH 6.0; 0.1 M phosphate buffer, pH 8.0; PBS, pH 7.4; 0.025 M MES buffer, pH 5.0; and 0.1 M Tris−HCl buffer, pH 7.2.

2.3 | Preparation of the immunoplatforms

A 3-μL aliquot of HOOC-MBs was transferred into a 1.5-mL Eppendorf tube and washed twice with 50 μL of MES buffer solution, pH 5.0, for 10 min while shaking (25 °C, 950 rpm). MBs were placed in the magnetic concentrator for 3 min before removing the supernatant after each washing step. Thereafter, HOOC-MBs were activated through their incubation in a mixture solution containing EDC and sulfo-NHS (50 mg/mL each in MES buffer solution) under continuous stirring at room temperature (25 °C, 950 rpm) for 35 min. Once washed twice with 50 μL of MES buffer solution, the activated MBs were incubated for 15 min in the specific antibody solution (25 μL of 2.5 μg/mL in MES buffer solution, 25 °C, 950 rpm). The remaining HOOC-activated groups were blocked by incubating the MBs with 25 μL of a 1.0 M ethanolamine solution (made in phosphate buffer pH 8.0) for 1 h (25 °C, 950 rpm). The as-modified MBs were washed with 0.1 M Tris-HCl buffer (pH 7.2) and twice with PBS and stored at 4 °C in sterilized PBS until their use.

The GAS6 sandwich immunocomplexes were formed by incubating the CAb-MBs in 25 μL of a solution containing the GAS6 standard (or the sample to be analyzed) for 45 min (25 °C, 950 rpm). After two washings with casein blocking buffer solution (BB), the immunoconjugates were incubated in a solution containing 2.5 μg/mL of b-DAb for 15 min (25 °C, 950 rpm), followed by a labelling step through incubation with 25 μL of a 1/1000 Strep-HRP solution prepared in BB solution for 15 min. Finally, the sandwich MBs-immunocomplexes were washed twice and re-suspended in 50 μL of 0.05 M phosphate buffer, pH 6.0, to perform the amperometric measurements.

2.4 | Amperometric measurements

Once a new SPCE was placed in the PMMA casing, the modified-MBs suspension was drop-casted onto the WE

RESEARCH ARTICLE
doi.org/10.1002/elsa.202100096
Chemistry Europe
European Chemical Societies Publishing

surface. The magnet holding block/SPCE ensemble was connected to the potentiostat through the specific cable and immersed into an electrochemical cell containing 10 mL of 0.05 M phosphate buffer, pH 6.0, supplemented with 1.0 mM HQ (freshly prepared). Amperometric measurements were recorded at − 0.20 V (vs. Ag pseudoreference electrode) under continuous stirring by adding 50 μL of a recently prepared 0.1 M H_2O_2 solution. The amperometric signals given through the manuscript correspond to the difference between the steady-state and the background currents and, unless otherwise stated, are the average values of three replicates of the amperometric signals provided by different bioplatforms prepared in the same way, and thus comprising the full modification of MBs with sandwich immunoconjugates and the amperometric transduction at SPCEs. Error bars were estimated as triple of the standard deviation of these replicates (confidence intervals calculated for $\alpha = 0.05$).

2.5 | Application to the analysis of biological samples

The developed immunosensor was applied to the determination of the GAS6 circulating level in plasma from patients of HF or pancreatic cancer, and in secretomes of human CRC cell lines.

The plasma samples from control individuals and patients diagnosed with HF and PDAC were provided by the Institut d'Investigacions Biomèdiques August Pi I Sunyer (IDIBAPS) and Hospital del Mar Medical Research Institute (IMIM), respectively, with the corresponding ethical permissions (IDIBAPS 2009/4729; IMIM 2020/9067/I), and the informed consent from all the involved individuals.

The determination, after verification of a matrix effect, was carried out by applying the standard additions method, adding increasing concentrations of GAS6 standards (500−2000 pg/mL) to the 1/50 diluted plasma samples.

The results obtained with the immunoplatform were compared with those provided by the ELISA method using the same immunoreagents and the protocol described by Muñoz-San Martín et al.,[31] with the following reagent concentrations: 400 ng/mL CAb solution (prepared in PBS), 100 ng/mL b-DAb solution (in Reagent Diluent solution), and Strep-HRP prepared by diluting 200 times the solution provided in the commercial kit with Reagent Diluent solution. In this case, increasing concentrations of GAS6 standards (20−80 pg/mL) were added to 200-times diluted plasma samples to perform the determination.

SW480 and SW620 cell lines from the same patient, the first one derived from the primary site of CRC and the second from the recurrent lymph node metastasis, were purchased from the American Type Culture Collection (ATCC) cell repository, and KM12C, KM12SM, and KM12L4a from I. Fidler's laboratory, MD Anderson Cancer Center, Houston, TX. Cells were grown and lysed following the protocols previously described.[32] The secretomes were prepared by seeding the cells at confluence and cultured at 37 °C in a 5 % CO_2 atmosphere for 48 h in DMEM with 10 % fetal bovine serum. Thereafter, they were washed with PBS, incubated 1 h in DMEM fetal bovine serum-free medium, washed again with PBS and cultured for 48 h under the same conditions in DMEM fetal bovine serum-free medium. Next, the conditioned medium (secretome) was harvested, centrifuged at 1500 × g to remove cell debris, aliquoted and stored at −80 °C until use.[20]

Cell secretomes were analyzed crude with the immune platform, using the same protocol detailed for GAS6 standards in sections 2.3 and 2.4, and by WB, in this case after preconcentration 60 times.

3 | RESULTS AND DISCUSSION

This work reports the first electrochemical immunosensor to date for the determination of GAS6. The bioplatform involves the selective capture of the target protein by a primary antibody (CAb) immobilized on the surface of HOOC-MBs. The target GAS6 was subsequently sandwiched with a biotinylated secondary antibody (b-DAb) further labeled with a Strep-HRP polymer. Once the MBs bearing the immunoconjugates were magnetically captured on the surface of the SPCEs, the electrochemical detection was carried out by monitoring the cathodic current measured at − 0.20 V vs. the Ag pseudoreference electrode using the H_2O_2/HQ system.[33,34] All the steps involved in the immunoplatform design and the reactions implicated in the amperometric measurements are shown in Figure 1.

3.1 | Optimization of working variables

The experimental variables involved in the preparation of the developed immunoplatform were optimized. A better signal-to-blank ratio (S/B) measured at −0.20 V in the presence (S) of 1.0 ng/mL GAS6 standard and in its absence (B) was used as selection criterion for each variable. The tested variables as well as the selected values are summarized in Table 1 and the corresponding experimental results are displayed in Figure 2.

Figure 2A shows a significant increase of the S/B ratio up to a CAb concentration of 2.5 μg/mL, levelling off for larger concentrations, which is probably due to the CAb

RESEARCH ARTICLE
doi.org/10.1002/elsa.202100096
Chemistry Europe
European Chemical Societies Publishing

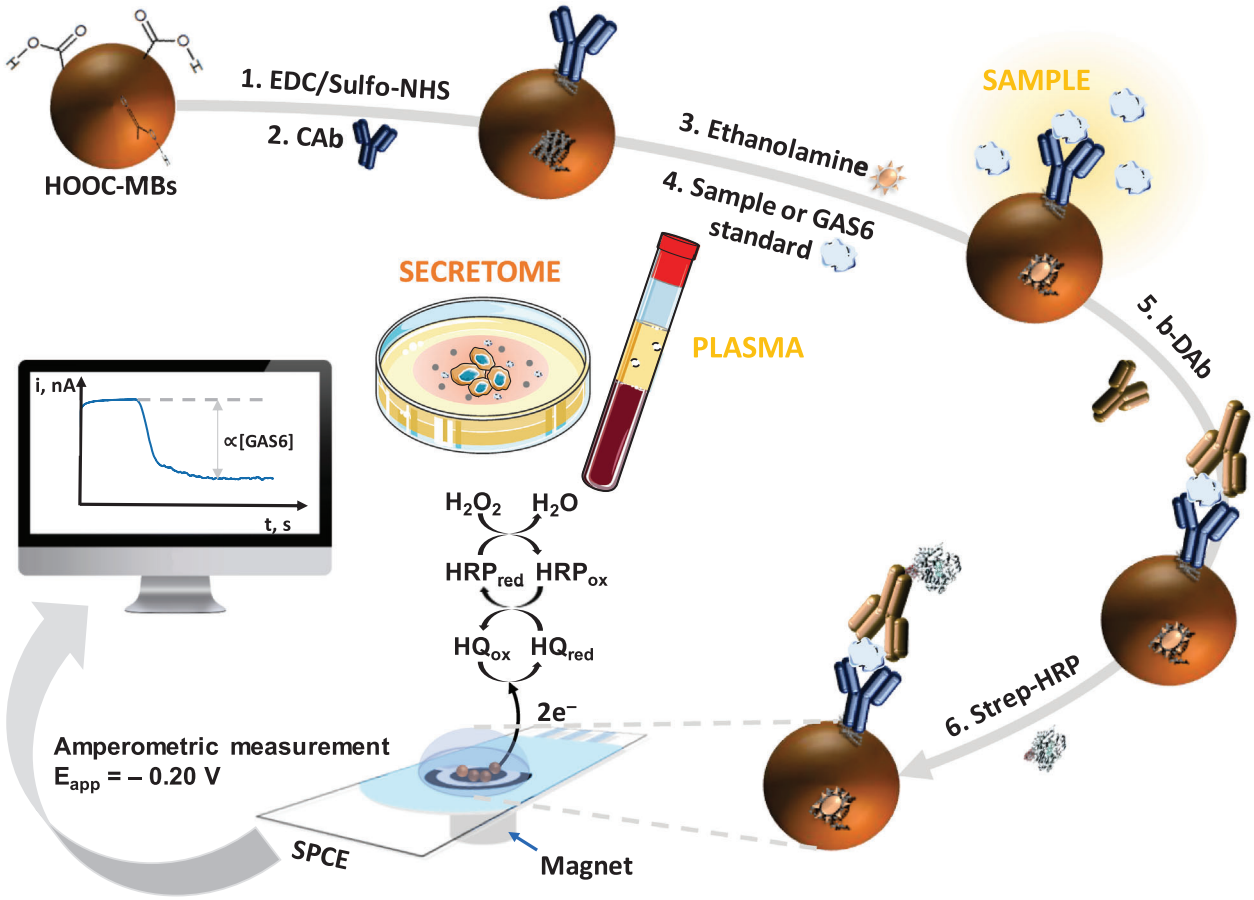

FIGURE 1 Scheme displaying the experimental procedure followed for preparing the MBs-based immunosensor for the determination of GAS6, by forming HRP-labeled sandwich immunocomplexes involving specific capture and biotinylated detector antibodies, and Strep-HRP, and the reactions involved in the amperometric transduction at SPCEs using the H_2O_2/HQ system

TABLE 1 Optimization of the working variables involved in the preparation and functioning of the immunosensor developed for the determination of GAS6

Experimental variable	Tested range	Selected value
V_{MBs} (μL)	1 – 6	3
[CAb] (μg/mL)	0.0 – 50.0	2.5
CAb incubation time (min)	0 – 60	15
Number of assay steps	1 – 3	3
GAS6 incubation time (min)	0 – 60	45
[b-DAb] (μg/mL)	0.0 – 10.0	2.5
b-DAb incubation time (min)	5 – 60	15
Strep-HRP dilution	1/5,000 – 1/250	1/1,000
Strep-HRP incubation time (min)	0 – 60	15

saturation on the MBs surface. Moreover, it was not possible to discriminate the presence of the target protein in the absence of CAb (bars at 0 in Figure 2A) according to the sandwich immunoassay strategy employed (see Figure 1). In addition, 15 min was selected as the CAb immobilization time because of the larger S/B ratio observed (Figure 2B). With the aim of improving the efficiency of the methodology, different working protocols were tested: (A) three sequential incubation steps of the CAb-MBs in GAS6 (30 min), b-DAb (30 min), and Strep-HRP (5 min)

RESEARCH ARTICLE
doi.org/10.1002/elsa.202100096
Chemistry Europe
European Chemical Societies Publishing

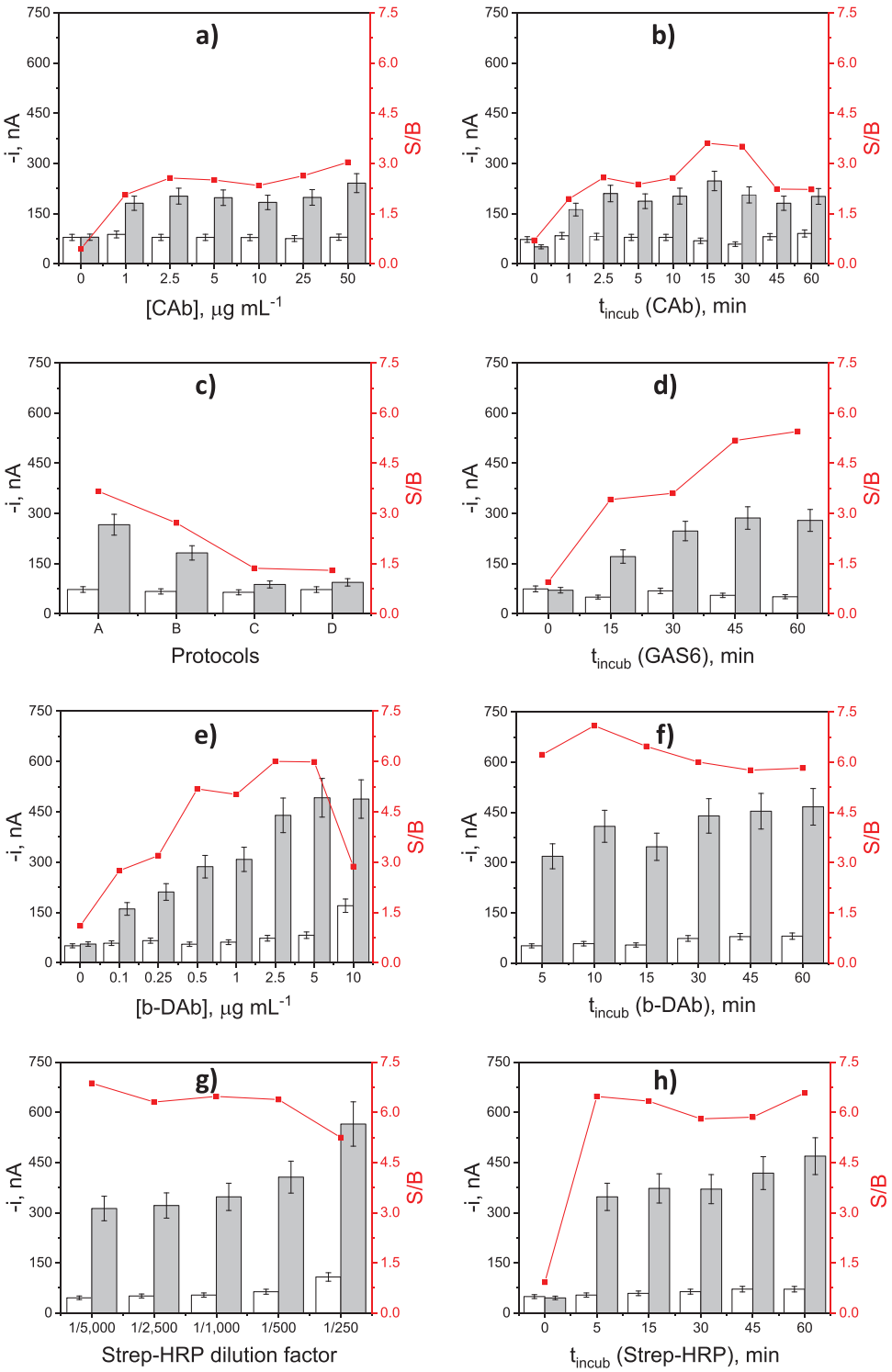

FIGURE 2 Optimization of the working variables involved in the preparation of the immunosensor developed for the determination of GAS6: CAb concentration (A), CAb incubation time (B), number of immunoassay steps (see main text) (C), GAS6 incubation time (D), b-DAb concentration (E), and incubation time (F), Strep-HRP dilution (G), and incubation time (H). Effect of each experimental variable on the amperometric signals measured with the immunosensors for 0.0 (white bars) and 1.0 (grey bars) ng/mL of GAS6 standard solutions, and the resulting signal-to-blank ratios (S/B, red lines)

RESEARCH ARTICLE
doi.org/10.1002/elsa.202100096
Chemistry Europe
European Chemical Societies Publishing

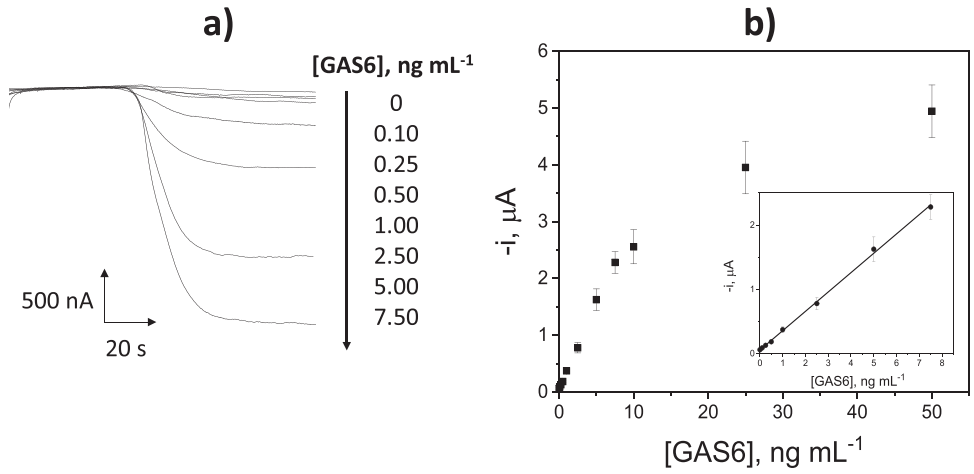

FIGURE 3 Real amperometric traces recorded (A), and calibration curve (B) obtained for the amperometric determination of increasing GAS6 standards concentrations using the developed immunoplatform. Inset in (B), linear calibration plot

solutions, respectively; (B) two sequential steps involving a 30 min incubation step of the CAb-MBs in GAS6 standard solution followed by another 30 min incubation period in a mixture solution of b-DAb and Strep-HRP; (C) two sequential incubation steps of the CAb-MBs in a mixture solution of GAS6 and b-DAb (30 min) followed by another 30 min incubation in the Strep-HRP solution, and (D) a single 30 min incubation step in a mixture solution containing GAS6, b-Dab, and Strep-HRP. Figure 2C shows as larger S/B ratio was obtained when using the 3-step working protocol (protocol A), probably due to a worse immunological target recognition by b-DAb after Strep-HRP labeling or to agglutination events resulting when working with immunoreagents mixture solutions. Therefore, protocol A was selected for the development of the immunosensor. Figure 2D shows no significant difference in the S/B ratio for GAS6 incubation time longer than 45 min, so that this value was selected for GAS6 capture by the CAb-MBs. The effect of b-DAb concentration, displayed in Figure 2E, showed an increase in the S/B ratio with such concentration up to 2.5 μg/mL. The ratio decreased for concentrations larger than 5 μg/mL probably caused by agglutination events that occur in homogeneous solutions, leading to an increase of the non-specific adsorptions. Although a 10 min incubation in the b-DAb solution provided larger S/B ratio (Figure 2F), a 15 min period was selected because of the lower experimental error. Moreover, a 1/1000 dilution of Strep-HRP (Figure 2G) and a labeling time of 15 min (Figure 2H) were selected.

3.2 | Analytical characteristics

Figure 3A shows some representative amperometric signals obtained with the developed immunosensor for different GAS6 concentrations under the selected experimental conditions. The measured response increased linearly with the GAS6 concentration over the 0.09 to 7.50 ng/mL range (inset in Figure 3B), according to the equation: $-i\ (nA) = (300 \pm 10)\ [GAS6]\ (nA\,ng^{-1}\,mL) + (60 \pm 40)\ (nA)$; $R^2 = 0.9986$. The limit of detection (LOD) was estimated following the $3 \times s_b/m$ criterion, where s_b was the standard deviation for 10 measurements carried out in the absence of GAS6, and m was the slope of the linear calibration plot (inset in Figure 3B). The calculated LOD value is 27 pg/mL, well below the levels of the target protein in plasma of healthy subjects (13–28 ng/mL)[35] and in patients with acute coronary syndrome (5.7–27.5 ng/mL)[35] and oral squamous cell carcinoma (28 ± 7 ng/mL).[36] The immunosensor showed high reproducibility for the measurements (RSD = 3.9 % by testing the amperometric signals provided by 10 different bioplatforms for a 5.0 ng/mL GAS6 standard) and a reduced time of analysis of 75 min. In addition, the storage stability of the prepared magnetic immunoconjugates (CAb-MBs stored in filtered PBS at 4 °C upon their preparation) was checked. The comparison of the amperometric responses measured each control day for 0.0 and 4.0 ng/mL of GAS6 standards showed that the immunoconjugates could be stored only for 3 days without significant loss of sensitivity.

The lack of other reported electrochemical immunosensors for the determination of GAS6 does not make it possible to compare the performance of the developed immunosensor with that provided by other electrochemical strategies. However, the usual method to measure levels of GAS6 in human plasma is a sandwich ELISA. ELISA methods claimed LOD values of 5.9 ng/mL[37] and 0.26 ng/mL,[38] remarkably higher than that achieved with the electrochemical immunosensor (27 pg/mL). Nevertheless, there are several commercially available ELISA

RESEARCH ARTICLE
doi.org/10.1002/elsa.202100096
Chemistry Europe
European Chemical Societies Publishing

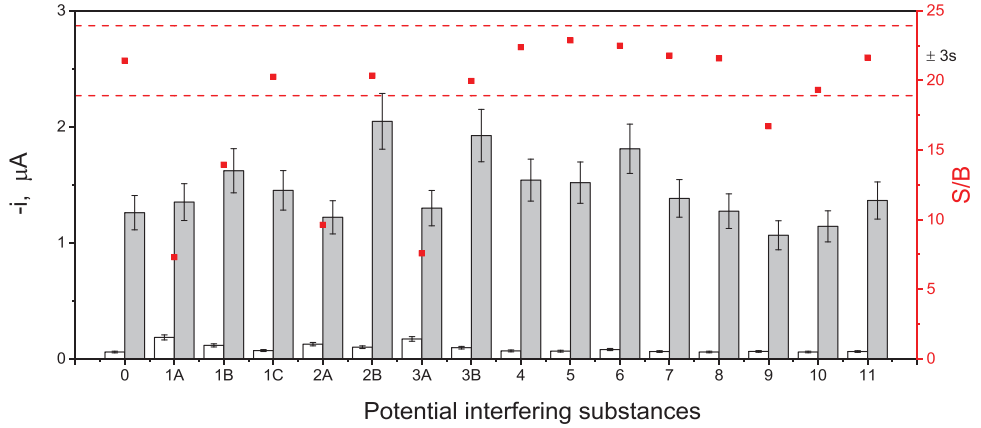

FIGURE 4 Effect of potential interferents. Amperometric responses obtained with the developed immunosensor for 0.0 (white bars) and 4.0 (grey bars) ng/mL GAS6 standards (and the corresponding S/B ratio, red squares) prepared in the absence (0) or in the presence of potentially interfering proteins: 1.0, 0.1, and 0.01 mg/mL human IgG (1A–C), 5.0 and 0.5 mg/mL Hb (2A-B), 50.0 and 5.0 mg/mL HSA (3A–B), 450 pg/mL NT-proBNP (4), 70 ng/mL Axl (5), 300 μg/mL Lp(a) (6), 10 ng/mL TNF-α (7), 500 ng/mL CDH-17 (8), 10 ng/mL E-CDH (9), 460 pg/mL HIF-1α (10), and 50 ng/mL IL-13Rα2 (11)

methods for GAS6 claiming LODs ranging between 0.65 and 125 pg/mL, which are comparable to that reported in this work (27 pg/mL). However, the achieved sensitivity is sufficient for GAS6 determination, since the GAS6 level for healthy individuals is reported between 13 and 28 ng/mL[35]), in a notably shorter assay time (75 min counting form the preparation of the CAb-MBs versus 4 h once the CAb-plate is prepared and blocked with ELISA tests) and using nonexpensive instrumentation, hardly portable and able to be miniaturized. It is important to mention that the ELISA methodology is limited to the determination of a single biomarker whereas major advances in both instrumentation and screen-printed electrodes allow multi-determinations of 2, 4, 8, and even 96 biomarkers using electrochemical multiplexing platforms.

Jaksch-Bogensperger et al. developed a methodology for the determination of GAS6 based on the Proseek method, which is a reagent Kit system (Olink Bioscience) to detect and quantify proteins in samples like serum and plasma, based on the Proximity Extension Assay (PEA) technology for single protein detection and a proximity-dependent DNA polymerization event, combined with the use of real-time PCR.[39] The authors reported a better sensitivity than that of the ELISA method using the same immunoreagents (1 pg/mL vs. 125 pg/mL, respectively). Compared with the electrochemical immunoplatform, it is important to mention the simplicity of the developed immunoplatform since it does not require complex antibody modifications, and expensive reagents and instrumentation. All the mentioned advantageous features make the electrochemical immunosensor a suitable tool for routine fast determination of GAS6 both in an individual or multiplexed way.

3.3 | Selectivity

The selectivity of the developed immunosensor was checked by comparing the amperometric responses measured for 0.0 and 4.0 ng/mL GAS6 standard solutions prepared in the absence and in the presence of some potential interfering proteins found in human serum: 1.0, 0.1, and 0.01 mg/mL human IgG, 5.0 and 0.5 mg/mL Hb, 50.0 and 5.0 mg/mL HSA, 450 pg/mL NT-proBNP, 70 ng/mL Axl, 300 μg/mL Lp(a), 10 ng/mL TNF-α, 500 ng/mL CDH-17, 10 ng/mL E-CDH, 460 pg/mL HIF-1α and 50 ng/mL IL-13Rα2.

The results displayed in Figure 4 show similar S/B ratios to that obtained for GAS6 in the presence of NT-proBNP (bars 4), Axl (bars 5), Lp(a) (bars 6), TNF-α (bars 7), CDH-17 (bars 8), HIF-1α (bars 10), and IL-13Rα2 (bars 11), indicating the absence of significant interference. Moreover, a slightly different response was observed in the presence of E-CDH (bars 9), suggesting a small interference from this nontarget protein. However, the presence of IgG (bars 1A–1C), Hb (bars 2A and 2B), and HSA (bars 3A and 3B) did affect notably the amperometric measurements for the larger concentrations assayed. The presence of circulating human antibodies reactive with animal proteins (human anti-animal antibodies, HAAA) can be associated with the interference observed in the presence of human IgG.[40] The interference found in the presence of Hb (Figure 4, bars 2A) can be attributed to its peroxidase activity.[41] Nevertheless, when the Hb concentration was 10 times lower (5.0 mg/mL), although both the nonspecific and specific signals are higher compared to those obtained in its absence (bars 2B vs. bars 0 in Figure 4), the calculated

RESEARCH ARTICLE
doi.org/10.1002/elsa.202100096
Chemistry Europe
European Chemical Societies Publishing

S/B ratio remained within the control limits set at ± 3 times the standard deviation of the S/B ratio calculated for GAS6. The effect of HSA has been described for other sandwich immunoassays when using HSA concentrations above 5 mg/mL,[42] since, unless it is highly purified, it can contain IgGs with a wide range of specificities that can disturb the assay (Figure 4, bars 3A and 3B). Importantly, these potential interferences did not hinder the usefulness of the developed immunosensor for the determination of GAS6 in the analyzed biological samples as it will be shown in the next section.

Moreover, in accordance with the DY885B DuoSet® ELISA specifications, 50 ng/mL of Axl/Fc Chimera, Dtk/Fc Chimera, and GAS1 Mer/Fc Chimera exhibited no interference with the antibodies involved in the immune platform and a sample containing 25 ng mL^{-1} of recombinant mouse GAS6 showed 0.3% of cross-reactivity.

3.4 | GAS6 expression in cell secretomes and determination in plasma samples from HF and cancer patients

The developed immunoplatform was applied to assess GAS6 expression in raw secretomes of isogenic pairs of colorectal cancer cells. Figure 5A) shows that the amperometric responses were larger than that of the blank for KM12C, KM12SM, KM12L4a, and SW480 and significantly much larger for SW620 secretomes. These results reflect that SW620 cells are highly tumorigenic and metastatic in comparison with the isogenic primary cell line SW480 and secrete much more GAS6 than the other cells. This agrees with that observed by WB (Figure 5C). It is important to note the much poorer sensitivity of WB compared with the immunosensor. Indeed, the WB detection of GAS6 in the SW480 secretome was not feasible (see caption of Figure 5C).

Regarding the determination of GAS6 in plasma, the potential existence of a matrix effect was checked by comparing the slope values of the calibration plots constructed with GAS6 standard solutions (300 ± 10 nA mL ng^{-1}) and with representative 50-times diluted plasma samples from a healthy individual (230 ± 20 nA mL ng^{-1}; t_{exp} = 9.124) and HF (160 ± 40 nA mL ng^{-1}; t_{exp} = 5.303) and PDAC (117 ± 2 nA mL ng^{-1}; t_{exp} = 19.780) patients with increasing concentrations of GAS6 standards (500–2000 pg/mL) added. The Student's *t*-test showed that statistically significant differences between the slope values were found for all the plasma samples ($t_{exp} > t_{tab} = 2.776$).

Therefore, due to the existence of matrix effect in plasma and the inter variability of these matrices, the determination was performed by applying the standard additions method. The obtained results are summarized in Table 2 and displayed, grouped by pools, in Figure 6A). These results agree with those reported in the literature for healthy subjects (13–28 ng/mL[43]), patients with acute coronary syndrome (5.7–27.5 ng/mL[43]) and patients with oral squamous cell carcinoma (28 ± 7 ng/mL[36]). Figure 6A shows as the circulating levels of GAS6 are not significantly different in HF patients but they are for PDAC patients, which agrees with that reported for HF patients[44] and with the overexpression of GAS6 in PDAC-derived cell lines.[9,45]

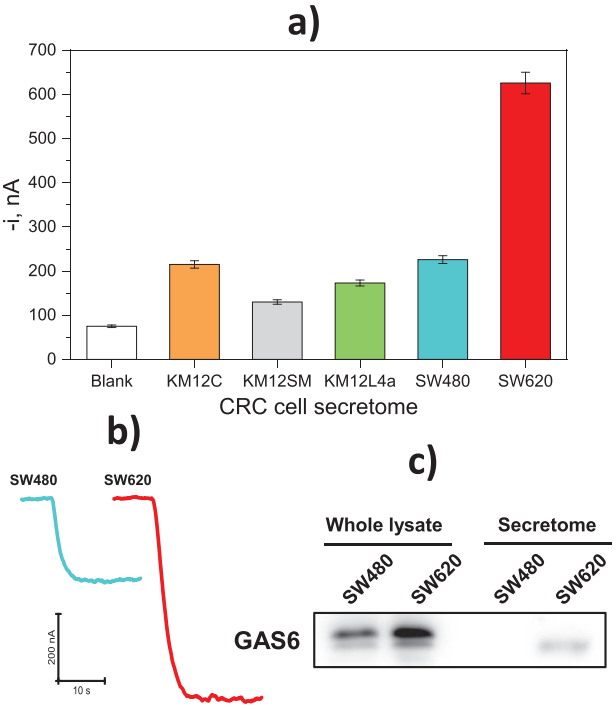

FIGURE 5 Assessment of GAS6 expression in human CRC cell secretomes. Amperometric responses (A) and representative amperometric traces (B) provided by the immune platform in the analysis of raw secretomes. WB analysis of 10 μg raw cell lysates and secretomes (60 times more concentrated than with the immunosensor) separated by 10% SDS-PAGE, transferred to nitrocellulose membranes, and proved with the GAS6 polyclonal antibody specified in section 2.2

The statistical comparison of the concentrations determined with the developed immunoplatform and the ELISA methodology showed that there were not significant differences for the results provided by both methods ($t_{exp} < t_{tab} = 2.776$; $\alpha = 0.05$ for results shown in Table 2, and slope and intercept values of (0.97 ± 0.06) and (1 ± 2) ng/mL including the unit and the zero values, respectively, for the correlation plot displayed in Figure 6B).

These obtained results demonstrate the practical usefulness of the developed strategy to assist in the differential analysis of cancer secretome, which is addressed for the first time in the literature with an electrochemical

doi.org/10.1002/elsa.202100096

TABLE 2 GAS6 concentrations (in ng/mL) provided by the immune platform and with the ELISA methodology in plasma samples of HF and PDAC patients

		Immune platform		ELISA			
Subjects	**Sample**	**[GAS6]**	**$RSD_{n=3}$ (%)**	**[GAS6]**	**$RSD_{n=3}$ (%)**	t_{exp}	t_{tab}
Healthy individuals	1	22 ± 4	7.4	22 ± 4	6.8	0.487	2.776
	2	18.4 ± 0.8	1.6	19 ± 4	8.1	0.415	
	3	18 ± 4	9.5	17.0 ± 0.5	1.3	1.280	
	4	19 ± 1	2.5	17 ± 4	10.0	1.603	
	5	20 ± 3	5.1	21 ± 3	6.3	0.727	
	6	21 ± 3	6.4	21 ± 5	9.6	0.005	
HF patients	7	33 ± 5	5.6	32 ± 2	2.0	0.898	
	8	20 ± 2	4.6	21 ± 5	9.4	1.244	
	9	22 ± 3	5.0	22 ± 3	5.7	0.130	
	10	22 ± 3	4.9	22 ± 1	1.7	1.446	
	11	19 ± 4	7.6	20 ± 3	5.8	1.004	
PDAC patients	12	45 ± 4	3.8	46 ± 7	5.8	0.333	
	13	20 ± 3	6.3	20 ± 2	5.0	0.463	
	14	45 ± 5	4.8	45 ± 9	8.2	0.055	
	15	35 ± 6	6.7	33 ± 8	9.6	0.879	
	16	44 ± 4	3.9	45 ± 4	3.9	0.436	

*(mean value $\pm t \times s/\sqrt{n}$).

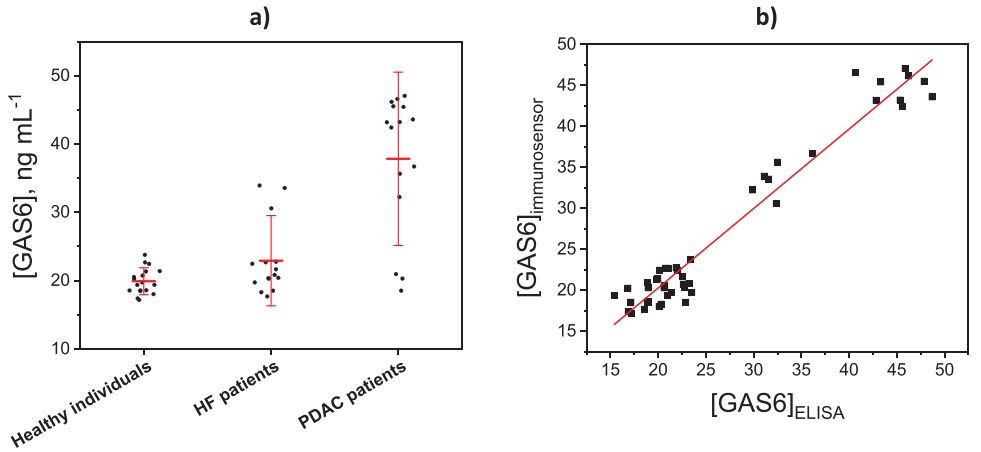

FIGURE 6 (A) Circulating GAS6 concentrations (in ng/mL) measured with the developed immune platform in plasma samples grouped into pools of healthy individuals, HF and PDAC patients. (B) Correlation plot of the GAS6 concentration values provided by the developed immune platform and the ELISA methodology in the 16 plasma samples analyzed (the three replicates performed for each analyzed sample have been considered for correlation)

biosensor, as well as to a minimally invasive diagnosis of PDAC, one of the most aggressive tumors in humans and the fourth higher cause of cancer mortality in Europe.[46]

4 | CONCLUSIONS

This work reports the development of the first electrochemical immune platform for the suitable determination of the GAS6 protein in plasma of patients with high prevalence and mortality diseases as well as for assessing the GAS6 expression in cancer cell secretomes.

The developed biosensor involves the selective capture of the target protein by micromagnetic immunoconjugates, and the GAS6 sandwiching with a biotinylated secondary antibody further labeled with a Strep-HRP conjugate. The electrochemical detection is carried out by amperometry at SPCEs using the HQ/H_2O_2 system.

The analytical performance of the immune platform makes it appropriate for clinical application. Moreover, the good reproducibility of the measurements and a reduced time of analysis of 75 min are other important practical advantages of the developed strategy. Importantly, the obtained results in the analysis of plasma samples statistically agree with those obtained by using the ELISA method, but at lower cost and in less time, thus suggesting the potential of the immune platform the rapid assessment of cancer secretome and the minimally invasive diagnosis of PDAC, predicted to become the second leading cause of cancer mortality by 2030.[47]

ACKNOWLEDGMENTS

This work is part of the POSITION-II project funded by the ECSEL Joint Undertaking under grant number Ecsel-783132-Position-II-2017-IA; www.position-2.eu, and PCI2018-093067 (Spanish Ministerio de Ciencia e Innovación) to M.P. The financial support of PID2019-103899RB-I00 (Spanish Ministerio de Ciencia e Innovación) Research Project to S.C., PI17CIII/00045 and PI20CIII/00019 grants from the AES-ISCIII program to R.B. and the TRANSNANOAVANSENS-CM Program from the Comunidad de Madrid (Grant S2018/NMT-4349) to S.C., RTI2018-095672-B-I00 (Spanish Ministerio de Ciencia e Innovación) to P.G.F.; Fundació la Marató de TV3 project 081010 to M.B.; research project PI20/00625, from the AES-ISCIII/FEDER program, to P.N, are gratefully acknowledged. A. Montero-Calle acknowledges the support of the FPU predoctoral contracts by the Spanish Ministerio de Educación, Cultura y Deporte. G.S-F. is recipient of a predoctoral contract (grant number 1193818N) supported by The Flanders Research Foundation (FWO). C. Muñoz-San Martín acknowledges a predoctoral contract from Complutense University of Madrid. R.M. Torrente-Rodríguez acknowledges a Talento-Contract from Comunidad de Madrid (2019-T2/IND-15965).

DATA AVAILABILITY STATEMENT

The data that support the findings of this study are available from the corresponding authors upon reasonable request.

ORCID

Susana Campuzano https://orcid.org/0000-0002-9928-6613

REFERENCES

1. P. P. Sainaghi, M. Bellan, A. Nerviani, *Dis. Markers* **2021**, *2021*, 2854925.
2. E. D. Lew, J. Oh, P. G. Burrola, I. Lax, A. Zagórska, P. G. Través, J. Schlessinger, G. Lemke, *eLife* **2014**, *3*, e03385.
3. S. Laurance, C. A. Lemarié, M. D. Blostein, *Adv. Nutr.* **2012**, *3*, 196.
4. I. Balogh, S. Hafizi, J. Stenhoff, K. Hansson, B. Dahlbäck, *Arterioscler. Thromb. Vasc. Biol.* **2005**, *25*, 1280.
5. S. Takako, P. G. Knyazev, N. J. Clout, Y. Cheburkin, W. Göhring, A. Ulrich, R. Timpl, E. Hohenester, *EMBO J.* **2014**, *25*, 80.
6. J. H. van der Meer, T. van der Poll, C. van 't Veer, *Blood* **2014**,*123*, 2460.
7. J. Huckriede, S. Bülow Anderberg, A. Morales, F.de Vries, M. Hultström, A. Bergqvist, J. T. Ortiz, J. W. Sels, K. Wichapong, M. Lipcsey, M. van de Poll, A. Larsson, T. Luther, C. Reutelingsperger, P. García de Frutos, R. Frithiof, G. A. F. Nicolaes, *Research Square* **2020**, https://doi.org/10.21203/rs.3.rs-52432/v1
8. M. Hutterer, P. Knyazev, A. Abate, M. Reschke, H. Maier, N. Stefanova, T. Knyazeva, V. Barbieri, M. Reindl, A. Muigg, H. Kostron, G. Stockhammer, A. Ullrich, *Clin. Cancer Res.* **2008**, *14*, 130.
9. X. Song, H. Wang, C. D. Logsdon, A. Rashid, J. B. Fleming, J. L. Abbruzzese, H. F. Gomez, D.B. Evans, H. Wang, *Cancer* **2011**, *117*, 734.
10. S. Ammoun, L. Provenzano, L. Zhou, M. Barczk, K. Evans, D.A. Hilton,; S. Hafizi, C. O. Hanemann, *Oncogene* **2013**, *33*, 336.
11. S. J. Demarest, J. Gardner, M. C. Vendel, E. Ailor, S. Szak, F. Huang, A. Doern, X. Tan, W. Yang, D. A. Grueneberg, E. J. Richards, W. O. Endege, E. Harlow, L. A. Koopman, *Biochemistry* **2013**, *52*, 3102.
12. K. C. Chiu, C. H. Lee, S. Y. Liu, Y. T. Chou, R. Y. Huang, S. M. Huang, Y. S. Shieh, *Oral Oncol.* **2015**, *51*, 683.
13. W. Sun, J. Fujimoto, T. Tamaya, *Oncology* **2004**, *66*, 450.
14. M. Buehler, B. Tse, A. Leboucq, F. Jacob, R. Caduff, D. Fink, D.R. Goldstein, V. Heinzelmann-Schwarz, *Biomed. Res. Int.* **2013**, *2013*, 238284.
15. M. C. Abba, V. T. Fabris, Y. Hu, F. S. Kittrell, W. W. Cai, L. A. Donehower, A. Sahin, D. Medina, C. M. Aldaz, *Cancer Res.* **2007**, *67*, 4104.
16. A. M. Ibrahim, Z. Zane Gray, A. M. Gomes, L. Myers, F. Behbod, H. L. Machado, *NJP Precis. Oncol.* **2020**, *4*, 9.
17. H. Markus, K. Pjotr, A. Ariane, M. Reschke, H. Maier, N. Stefanova, T. Knyazeva, V. Barbieri, M. Reindl, A. Muigg, H. Kostron, G. Stockhammer, A. Ullrich, *Clin. Cancer Res.* **2007**, *14*, 130.
18. H. Xue, B. Lü, J. Zhang, M. Wu, Q. Huang, Q. Wu, H. Sheng, D. Wu, J. Hu, M. Lai, *J. Proteome Res.* **2010**, *9*, 545.
19. H. Xue, B. Lu, M. Lai, *J. Transl. Med.* **2008**, *6*, 52.
20. R. Barderas, M. Mendes, S. Torres, R. A. Bartolomé, M. López-Lucendo, R. Villar-Vázquez, A. Peláez-García, E. Fuente, F. Bonilla, J. I. Casal, *Mol. Cell Proteomics* **2013**, *12*, 1602.
21. R. L. Siegel, K. D. Miller, A. Jemal, *CA: A Cancer Journal for Clinicians* **2020**, *70*, 7.
22. A. A. Khorana, P. B. Mangu, J. Berlin, A. Engebretson, T. S. Hong, A. Maitra, S. G. Mohile, M. Mumber, R. Schulick, M. Shapiro, S. Urba, H. J. Zeh, M. H. G. Katz, *J Clin Oncol.* **2016**, *34*, 2541.
23. R.S. Robins, C.A. Lemarié, S. Laurance, M. N. Aghourian, J. Wu, M.D. Blostein, *Blood* **2013**, *121*, 692.
24. M. Tjwa,; L. Bellido-Martin, Y. Lin, E. Lutgens, S. Plaisance, F. Bono, N. Delesque-Touchard, C. Hervé, R. Moura, A. D. Billiau, C. Aparicio, M. Levi, M. Daemen, M. Dewerchin, F. Lupu, J. Arnout, J. M. Herbert, M. Waer, P. García de Frutos, B. Dahlbäck, P. Carmeliet, M.F. Hoylaerts, L. Moons, *Blood* **2008**, *111*, 4096.

25. M. D. Blostein, I. Rajotte, D. P. Rao, C. A. Holcroft, S.R. Kahn, *J. Thromb. Thrombolysis* **2011**, *32*, 272.
26. G.-X. Ruan, A. Kazlauskas, *J. Biol. Chem.* **2013**, *288*, 21161.
27. L. McShane, I. Tabas, G. Lemke, M. Kurowska-Stolarska, P. Maffia, *Cardiovasc. Res.* **2019**, *115*, 1286.
28. A. Tutusaus, M. Marí, J. T. Ortiz-Pérez, G. A. F. Nicolaes, A. Morales, P. García de Frutos, *Cells* **2020**, *9*, 2186.
29. F. S. Felix, L. Angnes, *Biosens. Bioelectron.* **2018**, *102*, 470.
30. A. Jones, L. Dhanapala, R. N. T. Kankanamage, C. V. Kumar, J. F. Rusling, *Anal. Chem.* **2020**, *92*, 345.
31. C. Muñoz-San Martín, M. Gamella, M. Pedrero, A. Montero-Calle, R. Barderas, S. Campuzano, J. M. Pingarrón, *Sens. Actuators B* **2020**, *307*, 127623.
32. A. Valverde, E. Povedano, V. Ruiz-Valdepeñas Montiel, P. Yáñez-Sedeño, M. Garranzo-Asensio, R. Barderas, S. Campuzano, J. M. Pingarrón, *Biosens Bioelectron*. **2018**, *117*, 766.
33. C. Camacho, J. C. Matías, B. Chico, R. Cao, L. Gómez, B. K. Simpson, R. Villalonga, *Electroanalysis* **2007**, *19*, 2538.
34. M. Eguílaz, M. Moreno-Guzmán, S. Campuzano, A. González-Cortés, P. Yáñez-Sedeño, J. M. Pingarrón, *Biosens. Bioelectron.* **2010**, *26*, 517.
35. L. Jiang, C. Y. Liu, Q. F. Yang, P. Wang, W. Zhang, *Am. J. Clin. Pathol.* **2009**, *131*, 738.
36. T. Jiang, G. Liu, L. Wang, H. Liu, *PLoS ONE* **2015**, *10*, e0133940.
37. S. Clauser, S. Peyrard, P. Gaussem, M. Crespin, J. Emmerich, M. Aiach, D. Borgel, *Clin. Chem.* **2007**, *53*, 1808.
38. F. Alciato, P. P. Sainaghi, L. Castello, L. Bergamasco, S. Carnieletto, G. C. Avanzi, *J. Immunoassay Immunochem.* **2008**, *29*, 167.
39. H. Jaksch-Bogensperger, A. Hammerschmid, L. Aigner, E. Trinka, R. Gehwolf, Y. Ebner, M. Hutterer, S. Couillard-Despres, *Biotech. Reports* **2018**, *18*, e00252.
40. S. E. F. Melanson, M. J. Tanasijevic, P. Jarolim, *Circulation* **2007**, *116*, e501.
41. D. V. Grigorieva, I. V. Gorudko, A. V. Sokolov, O. V. Kosmachevskaya, A. F. Topunov, I. V. Buko, E. E. Konstantinova, S. N. Cherenkevich, O. M. Panasenko, *Bull. Exp. Biol. Med.* **2013**, *155*, 118.
42. R. N. Zhao, Z. Feng, Y. N. Zhao, L. P. Jia, R.-N. Ma, W. Zhang, L. Shan, Q. W. Xue, H.S. Wang, *Talanta* **2019**, *200*, 503.
43. L. Jiang, C. Y. Liu, Q. F. Yang, P. Wang, W. Zhang, *Am. J. Clin. Path.* **2009**, *131*, 738.
44. G. Caldentey, P. García De Frutos, H. Cristóbal, M. Garabito, A. Berruezo, X. Bosch, R. San Antonio, E. Flores-Umanzor, R. J. Perea, T. M. De Caralt, J. Rodríguez, J. T. Ortiz-Pérez, *Eur. Heart J. Acute Cardiovasc. Care* **2019**, *8*, 708.
45. V. S. Pilli, A. Datta, A. Dorsey, B. Liu, R. Majumder, *Oncol. Rep.* **2020**, *44*, 1322.
46. M. Achalandabaso Boira, M. Di Martino, C. Gordillo, M. Adrados, E. Martín-Pérez, *BMC Cancer* **2020**, *20*, 909.
47. L. Rahib, B. D. Smith, R. Aizenberg, A.B. Rosenzweig, J. M. Fleshman, L. M. Matrisian, *Cancer Res*. **2014**, *74*, 2913.

How to cite this article: C. Muñoz-San Martín, V. Pérez-Ginés, R. M. Torrente-Rodríguez, M. Gamella, G. Solís-Fernández, A. Montero-Calle, M. Pedrero, V. Serafín, N. Martínez-Bosch, P. Navarro, P. García de Frutos, M. Batlle, R. Barderas, J. M. Pingarrón, S. Campuzano, *Electrochem. Sci. Adv.* **2021**, e2100096.
https://doi.org/10.1002/elsa.202100096